Defect Sites in H2-Reduced TiO2Convert Ethylene to High Density Polyethylene without Activator

UNIVERSITÀ DEGLI STUDI DI TORINO

Defect Sites in H_2-reduced-TiO_2 Convert Ethylene to High Density PolyEthylene without Activator

Caterina Barzan, Elena Groppo,* Silvia Bordiga and Adriano Zecchina

Department of Chemistry, INSTM and NIS Centre, University of Torino, Via Quarello 15 A, Torino 10135, Italy

ABSTRACT: We show the unprecedented potential of commercially available TiO_2 materials reduced in H_2 (H_2 reduced-TiO_2) in the conversion of ethylene to high density polyethylene (HDPE) under mild conditions (room temperature, low pressure, absence of any activator), with the consequent formation of HDPE/TiO_2 composites which have been characterized by electron microscopy. Combination of UV-Vis and IR spectroscopies allows to demonstrate that ethylene polymerization occurs on Ti^{4-n} defect sites, that behave as shallow-trap defects located in the band-gap and, differently from the active sites in the widely used Ziegler-Natta catalysts, do not contain any alkyl (Ti-R) neither hydride (Ti-H) ligands. These results might have interesting implications on the mechanism of ethylene polymerization and open valuable perspectives for commercial TiO_2 materials as catalysts for polyethylene production under mild conditions.

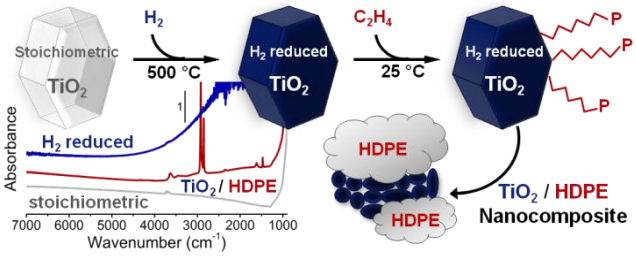

Keywords: H_2-reduced TiO_2, Ziegler-Natta catalysts, defect sites, ethylene polymerization, HDPE.

Titanium dioxide (TiO_2) is one of the most investigated material in the field of photocatalysis,[1] photovoltaics[2] (coupled with organic dies) and water splitting.[3] Defective TiO_2 is even more attractive compared to stoichiometric TiO_2 because of its narrower band gap (less than 3 eV) which allows the absorption of visible light and a moderate conductivity. Several approaches have been proposed in order to introduce defects into TiO_2, with the aim of engineering the band-gap and improving solar light harvesting. The most popular methods involve either the introduction of dopants (metals, non-metals[4-7] or self-dopant Ti^{3+} species[8]) or the generation of oxygen vacancies through annealing (outgassing at high temperatures in UHV)[9] or reduction in hydrogen atmosphere.[10,11] Recently, black TiO_2 nanoparticles with 1.0 eV band-gap were obtained through high pressure hydrogenation starting from crystalline TiO_2[1] and amorphous TiO_2,[12] respectively. The authors ascribe the observed color, and therefore the narrowed band-gap, to the synergistic presence of surface disorder and oxygen vacancies in bulk and surface positions. These black TiO_2 nanoparticles are highly stable in air for over 10 months, due to the replenishment of oxygen in the surface vacancies, leaving a unique crystallinity core/disordered shell morphology. Black TiO_2 shows enhanced photocatalytic activity with respect to stoichiometric TiO_2, *e.g.* in decomposition of methylene blue or for water splitting reaction upon irradiation with UV-Vis light. TiO_2 presenting surface and subsurface oxygen vacancies play also an active role in catalytic reactions involving the activation of water, alcohols, acetone and formaldehyde, without the need of light irradiation.[13-15]

In our prospect, the presence of Ti^{4-n} sites at the surface of reduced TiO_2 was attractive because of its similarity with the reduced Ti sites active in olefin polymerization and oligomerization. As a matter of fact, reduced Ti sites in interaction with an aluminum-alkyl activator are the active species in the well known $TiCl_x$-based heterogeneous Ziegler-Natta (ZN) catalysts,[16-19] which have a dominant share of polypropylene and polyethylene production. It is also known that $TiCl_2$ (where Ti has a +2 oxidation state) polymerizes ethylene in absence of any activator.[20] Finally, homogeneous aryloxy- and alkoxy-Ti^{2+} organometallic complexes selectively oligomerize ethylene to mainly 1-butene (Alphabutol process) and other light olefins.[21-24] Inspired by these examples and on the basis of our experience in the field of characterization of heterogeneous catalysts for ethylene polymerization,[25-32] we explored the potential of reduced TiO_2 materials in oligomerization/polymerization of ethylene. Herein, we report the first observation of the occurrence of ethylene polymerization undermild conditions (room temperature, low pressure, absence of any co-catalyst) at the surface of commercially available TiO_2 materials (Aldrich nanoanatase, nanorutile and Degussa P-25) reduced in H_2 atmosphere. We demonstrate that a high density polyethylene (HDPE) is obtained, characterized by a high degree of crystallinity.

Briefly, the activation procedure was as following: i) all TiO_2 samples were first degassed at 773 K in dynamic vacuum for several hours, followed by a treatment in oxygen at the same temperature (1 hour) in order to remove organic pollutants possibly present at the surface and to provide stoichiometric TiO_2 (hereafter, stoich-TiO_2); ii) a reduction step was carried out in hydrogen atmosphere (pressure of 200 mbar) at 773 K for 1 hour; iii) H_2 was pumped out at 773 K and the samples were rapidly cooled down to room temperature (hereafter, red-TiO_2). We would like to notice that the reduction conditions employed herein are milder than those leading to black-TiO_2 reported in literature, which require high H_2 pressure (more than 10 bars).[1] All the steps have been conducted in a quartz tube, in order to avoid possible contamination, as recently shown in literature.[33] All reduced samples show a blue color. At that point, ethylene was admitted into the reaction cell at room temperature and low pressure (lower than 200 mbar). A gradual decrease of ethylene equilibrium pressure was observed in all the cases, demonstrating that ethylene polymerization occurs. Remarkably, the kinetic behavior is reproducible upon new admission of ethylene for several times, testifying that the catalyst does not deactivate in the adopted experimental conditions. Reaction constants in the range of $5.0 \cdot 10^{-3}$ - $1.0 \cdot 10^{-2}$ $s^{-1}mol_{TiO2}^{-1}$ were obtained, corresponding to an activity of about 7 - 15 g_{PE} g_{TiO2}^{-1} h^{-1} at room temperature and low pressure. It should be noticed that the activity values refer to grams of catalyst and not to the amount of active sites, which are difficult to be estimated. The activity data evaluated from the kinetics of reaction were confirmed by analysis of the weight increase of the sample.

The observation of the reactivity of H_2-reduced TiO_2 materials towards ethylene under mild conditions prompted us to carry out a spectroscopic investigation to get information on the catalytic active sites and on the properties of the produced polymer. Hereafter, we will discuss in detail the results obtained on Degussa P-25 sample; similar results were obtained on nanoanatase and nanorutile samples, as reported in the Supporting Information. Figure 1a and b shows the DR UV-Vis-NIR (part a) and FT-IR (part b) spectra of stoichiometric P-25 (black curve, stoich-TiO_2), reduced in H_2 at 773 K (dark grey curve, red-TiO_2) and of H_2-reduced P-25 after ethylene polymerization at room temperature (bold light grey curve, red-TiO_2+C_2H_4). The spectra of stoichiometric P-25 (black curves) are basically flat over most of the frequency region, except above 26000 cm^{-1} (optical band-gap) and below 1000 cm^{-1} (bulk vibrational modes). The weak IR absorption bands observed around 3650 cm^{-1} are assigned to ν(O-H) of surface titanol species. The position and intensity of these bands differ as a function of sample (nanoanatase, nanorutile or Degussa P-25) and activation time.[34,35] Since titanols are not directly involved in ethylene polymerization reaction, these bands are not commented in details.

Upon H_2 reduction a broad and featureless absorption appears throughout the whole visible, NIR and MIR regions (dark grey spectra in Figure 1a and b), with a consequent drastic decrease in transmittance. This phenomenon has been widely studied[36-39] and is explained in terms of creation of shallow-trap defect sites (plausible Ti^{4-n} sites associated with oxygen vacancies) located in the band-gap. Electrons are promoted from these defect sites to the conduction band upon absorption of light. The closer is the defect to the valence band, the higher is the energy required to promote the electron in the conduction band. On the contrary, radiation in the IR region induces small thermal excitations that promote electrons from defect states which are close to the conduction band. A high density of states provides a continuum of electronic excitations, resulting in a featureless absorption in the whole IR region over a wide energy range (known as Drude absorption). Such a property of reduced TiO_2 was exploited to build up sensors for oxidizing/reducing agents:[40] as a matter of fact, an oxidizing/reducing asdorbate can remove/inject electrons into the surface defect states, inducing a change of the absorption in IR range. The effect of H_2 reduction on the UV-Vis-NIR and IR spectra is similar for the three TiO_2 materials investigated in this work (see SI), although some differences merit a comment. In particular, the broad Drude absorption is shifted at higher energy (i.e. wavenumber) values for nanorutile, suggesting that defect sites are electronically more profound (i.e. less close to the conduction band).

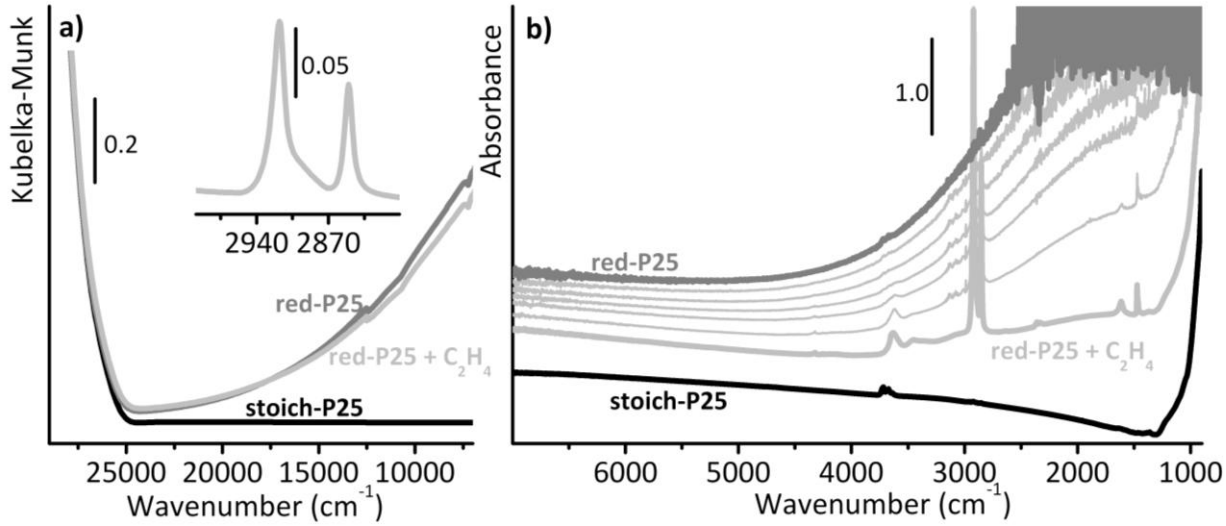

Figure 1. DR UV-Vis-NIR (part a) and FT-IR (part b) spectra of stoichiometric P-25 activated at 773 K in O_2 (bold black), reduced in H_2 atmosphere at 773 K (bold dark grey), and of the last sample after 12 hours of exposure to ethylene (bold light grey). The series of spectra in light grey colour are collected while ethylene polymerization occurs. Inset in part a) shows the IR spectrum (collected in ATR mode) in the $\nu(CH_2)$ region of the PE obtained on H_2-reduced P-25 during the DR UV-Vis measurement.

It is important to observe that the appearance of a broad absorption throughout the Vis-NIR-MIR region is the only spectroscopic phenomenon observed upon H_2-reduction of TiO_2 materials. No other absorption bands, which could reveal the presence of H-containing surface specie (e.g. Ti-H), are observed. The case of nanorutile is helpful in this context, since it is transparent in the 2500-1100 cm^{-1} region, where titanium hydride species are expected to contribute. Similarly, no additional absorption bands are observed in the IR spectrum of P25 only partially reduced in H_2 (i.e. treated in H_2 at 500°C for short contact time).

When ethylene interacts with reduced P-25, the broad absorption in the NIR-IR region due to the delocalized electrons slowly decreases in intensity, suggesting that a fraction of Ti^{4-n} sites are re-oxidized (light grey sequence of spectra in Figure 1b). This can be explained in terms of oxidative addition of ethylene to Ti^{4-n} sites, with consequent formation of Ti-R species (where R = alkyl chain), although a possible oxidant role of a few ppm of oxygen in the

ethylene feedstock cannot be ruled out. The phenomenon is much less evident in the UV-Vis region (Figure 1b), providing an evidence that re-oxidation involves defect sites close to the conduction band, much more than those electronically more profound. Simultaneously, IR absorption bands characteristic of polyethylene grow at 2923-2854 cm^{-1} (asymmetric and symmetric $\nu(CH_2)$) and at 1472-1459 cm^{-1} (asymmetric and symmetric $\delta(CH_2)$), revealing that H_2-reduced P-25 catalyzes ethylene polymerization. Hence, the decrease of ethylene pressure observed as a function of time, must be correlated with ethylene polymerization on the TiO_2 surface. Noticeably, no reaction takes place on stoichiometric TiO_2 under the same reaction condition, which means that the defect sites responsible for the ethylene polymerization are generated during the H_2-reduction treatment. The whole set of data discussed above suggest that the reaction likely occurs on defect sites electronically located in proximity of the conduction band, whereas those more profound in the band-gap are not involved.

A close inspection to the IR spectra allows to get information on the obtained polymer. Indeed, the absence of absorption bands due to CH_3 moieties ($\nu(CH_3)$ expected at 2965 and 2872 cm^{-1} and $\delta(CH_3)$ at 1379 cm^{-1}) is indicative of the formation of HDPE, a linear polymer with a negligible amount of branches. A polyethylene having the same vibrational spectrum is obtained during the DR UV-Vis experiment (as demonstrated by the IR spectrum collected in ATR mode on the same powder at the end of the UV-Vis experiment, inset of Figure 1a). The full width at high maximum and the intensity ratio between the absorption bands at 1472 and 1459 cm^{-1} (due to $\delta(CH_2)$) demonstrate that the obtained HDPE is highly crystalline, as confirmed by DSC data (see Figure S4).[41]

Finally, the morphology of the HDPE/TiO_2 composite material was investigated by HRTEM. A few representative images are shown in Figure 2. It is worth noticing that detection of a polymer phase on top of the regular TiO_2 crystals is not straightforward due to the poor contrast of the polymer with respect to TiO_2. At the adopted resolution, the H_2-reduced TiO_2 particles show a morphology and size distribution typical of Degussa P-25: the particles are regular and have polyhedral shapes, with flat terminations. Polyethylene is randomly distributed on top of the TiO_2 particles, forming an ill-defined phase (indicated by arrows in Figure 2). A throughout investigation of many regions of the sample revealed that polyethylene is present overall in the sample, most probably involving both anatase and rutile particles. This observation well matches with the fact that also reduced nano-rutile and nano-anatase (characterized by different type of defects: deeper in the band gap for nanorutile, closer to the conduction band for nanoanatase) showed to be active in ethylene polymerization (see SI). It is worth noticing that recent accurate HRTEM investigation have demonstrated that hydrogenated black TiO_2 nanocrystals show a crystalline-disordered core–shell structure.[42-44] However, the phenomenon observed herein contributes at a much larger dimensional scale: the "ill-defined phase" constitutes islands as large as 50 nm, which are by far much larger than the average dimension of TiO_2 particles.

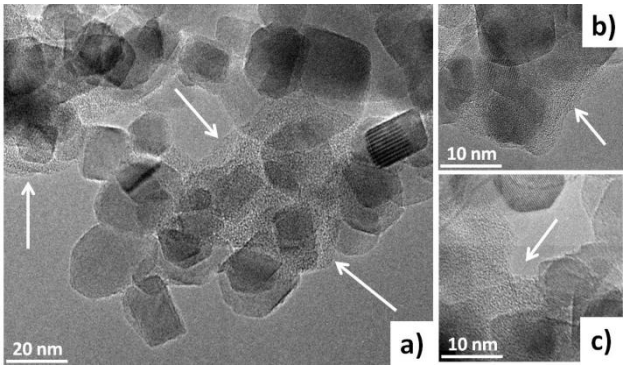

Figure 2. Representative HRTEM micrographs of H_2-reduced P-25 after ethylene polymerization occurred. Parts a), b) and c) report three different images representative of the whole sample; polyethylene phase is evidenced by white arrows.

In conclusion, the data shown herein demonstrate that commercially available TiO_2 samples can act as ethylene polymerization catalysts under mild conditions when reduced in H_2 at 773 K. Although the productivity is still low in comparison to the actually employed catalysts for ethylene polymerization, they have the advantage to be easy to be handled, non-toxic and widely available. Higher activity values could be achieved by increasing the fraction of active sites, for example with TiO_2 materials having a higher surface area, or by using other reducing methods; as well as by working at higher pressure and temperature. Therefore, the optimization of both, catalyst properties and reaction conditions offer promising perspectives in the field of polyethylene production. The exact nature and the amount of the active sites are still under investigation, but it can be safely stated that they are reduced Ti^{4-n} species that behave as shallow-trap defects located in the band-gap and are responsible of the appearance of a broad absorption in the whole Vis-NIR and MIR region. Interestingly, the active Ti sites differ from the majority of $TiCl_x$-based heterogeneous catalysts for ethylene polymerization in two main aspects: i) they do not have chlorine ligands in their coordination sphere, but only oxygen atoms; and ii) they polymerize ethylene without any activator. For this reason, H_2-reduced TiO_2 materials are comparable to the Cr/SiO_2 Phillips catalyst, where the active Cr-siloxy sites polymerize ethylene without any activator, and for which the mechanism of initiation reaction is still object of debate.[26,30,45,46] In the present case, the observation that a fraction of the Ti sites are re-oxidized during ethylene polymerization reaction and the absence of any evidence for Ti-H (or Ti-R) species, suggest that ethylene polymerization initiates through an oxidative addition. Future investigations will be devoted to the understanding of the reaction mechanism, with implications potentially useful to the whole community of researchers involved in olefin polymerization/oligomerization.

EXPERIMENTAL METHODS

The electronic and vibrational properties of stoichiometric TiO_2 (stoich-TiO_2) and reduced TiO_2 (red-TiO_2) samples were investigated by Diffuse Reflectance (DR) UV-Vis-NIR (Varian, Cary 5000) and transmission FT-IR (Bruker, Vertex 70) spectroscopy (Figure 1 and Figure S1). The same techniques were employed to monitor in situ the occurrence of ethylene polymerization, as frequently reported for other polymerization catalysts. The morphology of the TiO_2/polyethylene composite materials was determined by TEM (JEOL 3010-UHR, FigureS2), whereas the properties of the polymers were investigated by scanning electron microscopy (SEM, Zeiss evo50xvp, Figure S3) and differential scanning calorimetry (DSC, TA instrument Q200, Figure S4) techniques.

ASSOCIATED CONTENT

Supporting Information

Supporting Information Available: Vibrational and electronic spectra of H_2-reduced nanoanatase, nanorutile and P-25 reacted with ethylene, HR-TEM, SEM and DSC study of the TiO_2/HDPE composites. This material is available free of charge via the Internet at http://pubs.acs.org.

AUTHOR INFORMATION

Corresponding Author

*E-mail: elena.groppo@unito.it

AKNOWLEDGEMENTS

The work has been supported by FIRB (RBAP115AYN) and by Ateneo-Compagnia di San Paolo-2011-1A line, ORTO11RRT5 projects. The authors thank Federica Franconieri for HRTEM and SEM images, and Giuseppe Spoto along with Lorenzo Mino for useful discussion.

REFERENCES

(1) Chen, X. B.; Liu, L.; Yu, P. Y.; Mao, S. S., *Science* **2011**, *331*, 746-750.

(2) Wang, G. M.; Wang, H. Y.; Ling, Y. C.; Tang, Y. C.; Yang, X. Y.; Fitzmorris, R. C.; Wang, C. C.; Zhang, J. Z.; Li, Y., *Nano Lett.* **2011**, *11*, 3026-3033.

(3) Chen, X. B.; Shen, S. H.; Guo, L. J.; Mao, S. S., *Chem. Rev.* **2010**, *110*, 6503-6570.

(4) Hoffmann, M. R.; Martin, S. T.; Choi, W. Y.; Bahnemann, D. W., *Chem. Rev.* **1995**, *95*, 69-96.

(5) Chen, X. B.; Burda, C., *J. Am. Chem. Soc.* **2008**, *130*, 5018-5019.

(6) Livraghi, S.; Chiesa, M.; Paganini, M. C.; Giamello, E., *J. Phys. Chem. C* **2011**, *115*, 25413-25421.

(7) Bjorheim, T. S.; Kuwabara, A.; Norby, T., *J. Phys. Chem. C* **2013**, *117*, 5919-5930.

(8) Zuo, F.; Wang, L.; Wu, T.; Zhang, Z. Y.; Borchardt, D.; Feng, P. Y., *J. Am. Chem. Soc.* **2010**, *132*, 11856-11857.

(9) Thompson, T. L.; Yates, J. J. T., *Chem. Rev.* **2006**, *106*, 4428-4453.

(10) Rekoske, J. E.; Barteau, M. A., *J. Phys. Chem. B.* **1997**, *101*, 1113-1124.

(11) Barnard, A. S.; Zapol, P., *Phys. Rev. B* **2004**, *70*.

(12) Naldoni, A.; Allieta, M.; Santangelo, S.; Marelli, M.; Fabbri, F.; Cappelli, S.; Bianchi, C. L.; Psaro, R.; Dal Santo, V., *J. Am. Chem. Soc.* **2012**, *134*, 7600-7603.

(13) Panayotov, D. A.; Yates, J. T., *Chem. Phys. Lett.* **2005**, *410*, 11-17.

(14) Xia, Y. B.; Zhang, B.; Ye, J. Y.; Ge, Q. F.; Zhang, Z. R., *J. Phys. Chem. Lett.* **2012**, *3*, 2970-2974.

(15) Xu, M. C.; Noei, H.; Fink, K.; Muhler, M.; Wang, Y. M.; Woll, C., *Angew. Chem.-Int. Edit.* **2012**, *51*, 4731-4734.

(16) Albizzati, E.; Giannini, U.; Collina, G.; Noristi, L.; Resconi, L., *Catalysts and polymerizations*, in: Polypropylene Handbook; Moore, E. P. J., Ed.; Hanser-Gardner Publications: Cincinnati, OH, **1996**; Vol. Chapter 2.

(17) Mulhaupt, R., *Macromol. Chem. Phys.* **2003**, *204*, 289–327.

(18) Corradini, P.; Guerra, G.; Cavallo, L., *Acc. Chem. Res.* **2004**, *37*, 231-241.

(19) Busico, V., *Mrs Bulletin* **2013**, *38*, 224-228.

(20) Kissin, Y. V., *Alkene Polymerization Reactions with Transition Metal Catalysts*; Kissin, Y. V., Ed.; Elsevier, **2008**; Vol. 173.

(21) Suttil, J. A.; McGuinness, D. S., *Organometallics* **2012**, *31*, 7004-7010.

(22) Suttil, J. A.; McGuinness, D. S.; Pichler, M.; Gardiner, M. G.; Morgan, D. H.; Evans, S. J., *Dalton Trans.* **2012**, *41*, 6625-6633.

(23) McGuinness, D. S., *Chem. Rev.* **2011**, *111*, 2321-2341.

(24) Dixon, J. T.; Green, M. J.; Hess, F. M.; Morgan, D. H., *J. Organomet. Chem.* **2004**, *689*, 3641-3668.

(25) Groppo, E.; Seenivasan, K.; Barzan, C., *Catal. Sci. Technol.* **2013**, *3*, 858-878.

(26) Groppo, E.; Lamberti, C.; Bordiga, S.; Spoto, G.; Zecchina, A., *Chem. Rev.* **2005**, *105*, 115-183.

(27) Zecchina, A.; Groppo, E., *Proc. R. Soc. A-Math. Phys. Eng. Sci.* **2012**, *468*, 2087-2098.

(28) Groppo, E.; Damin, A.; Otero Arean, C.; Zecchina, A., *Chem. Eur. J.* **2011**, *17*, 11110 – 11114.

(29) Barzan, C.; Groppo, E.; Quadrelli, E. A.; Monteil, V.; Bordiga, S., *Phys.Chem.Chem.Phys.* **2012**, *14*, 2239–2245.

(30) Groppo, E.; Lamberti, C.; Bordiga, S.; Spoto, G.; Zecchina, A., *J. Catal.* **2006**, *240*, 172-181.

(31) Seenivasan, K.; Sommazzi, A.; Bonino, F.; Bordiga, S.; Groppo, E., *Chem. Eur. J* **2011**, *17*, 8648-8656.

(32) Seenivasan, K.; Gallo, E.; Piovano, A.; Vitillo, J. G.; Sommazzi, A.; Bordiga, S.; Lamberti, C.; Glatzel, P.; Groppo, E., *Dalton Trans.* **2013**, *42*, 12706-12713.

(33) Danon, A.; Bhattacharyya, K.; K., V. B.; Lu, J.; Sauter, D. J.; Gray, K. A.; Stair, P. C.; Weitz, E., *ACS Catal.* **2012**, *2* 45–49.

(34) Deiana, C.; Fois, E.; Coluccia, S.; Martra, G., *J. Phys. Chem. C* **2010**, *114*, 21531-21538.

(35) Mino, L.; Ferrari, A. M.; Lacivita, V.; Spoto, G.; Bordiga, S.; Zecchina, A., *J. Phys. Chem. C* **2011**, *115*, 7694-7700.

(36) Diebold, U., *Surf. Sci. Rep.* **2003**, *48*, 53-229.

(37) Szczepankiewicz, S. H.; Colussi, A. J.; Hoffmann, M. R., *J. Phys. Chem. B.* **2000**, *104*, 9842-9850.

(38) Szczepankiewicz, S. H.; Moss, J. A.; Hoffmann, M. R., *J. Phys. Chem. B.* **2002**, *106*, 2922-2927.

(39) Berger, T.; Sterrer, M.; Diwald, O.; Knozinger, E.; Panayotov, D.; Thompson, T. L.; Yates, J. T., *J. Phys. Chem. B.* **2005**, *109*, 6061-6068.

(40) Baraton, M. I.; Merhari, L., *Nanostruct. Mater.* **1998**, *10*, 699-713.

(41) Chelazzi, D.; Ceppatelli, M.; Santoro, M.; Bini, R.; Schettino, V., *Nat. Mater.* **2004**, *3*, 470-475.

(42) Xia, T.; Chen, X., *J. Mater. Chem. A* **2013**, *1*, 2983-2989.

(43) Liu, L.; Yu, P. Y.; Chen, X.; Mao, S. S.; Shen, D. Z., *Phys. Rev. Lett.* **2013**, *111*, Article n° 065505.

(44) Lu, H.; Zhao, B.; Pan, R.; Yao, J.; Qiu, J.; Luo, L.; Liu, Y., *RSC Adv.* **2014**, *4*, 1128-1132.

(45) McGuinness, D. S.; Davies, N. W.; Horne, J.; Ivanov, I., *Organometallics* **2010**, *29*, 6111-6116.

(46) Liu, B.; Nakatani, H.; Terano, M., *J. Mol. Catal. A* **2002**, *184*, 387-398.

Supporting Information for Publication

Defect Sites in H_2-reduced-TiO_2 Convert Ethylene to High Density PolyEthylene without Activator

Caterina Barzan, Elena Groppo,* Silvia Bordiga and Adriano Zecchina

Caterina Barzan
Department of Chemistry, INSTM and NIS Centre, University of Torino, Via Quarello 15 A, Torino 10135, Italy
caterina.barzan@unito.it

Elena Groppo
Department of Chemistry, INSTM and NIS Centre, University of Torino, Via Quarello 15 A, Torino 10135, Italy
elena.groppo@unito.it

Silvia Bordiga
Department of Chemistry, INSTM and NIS Centre, University of Torino, Via Quarello 15 A, Torino 10135, Italy
silvia.bordiga@unito.it

Adriano Zecchina
Department of Chemistry, INSTM and NIS Centre, University of Torino, Via Quarello 15 A, Torino 10135, Italy
adriano.zecchina@unito.it

1. Reactivity of H_2-reduced nanoanatase, nanorutile and P-25 towards ethylene: a comparison of vibrational and electronic spectra

FT-IR and DR-UV-Vis spectroscopies were useful tools to monitor the H_2-reduction (carried at 500 °C) of stoichiometric TiO_2 samples and to follow in-situ ethylene polymerization occurring at the surface of H_2-reduced TiO_2. Figure S1 shows DR-UV-Vis (parts a), c) and e)) and FT-IR (parts b), d) and f)) spectra, covering the whole MIR-NIR-Vis-UV range, of Aldrich nanoanatase (parts a) and b)), Aldrich nanorutile (parts c) and d)) and Degussa P-25 (parts e) and f)) samples.

All oxidized samples (black curves in Fig. S1) show a similar profile in the whole spectroscopic region. As far as concerns the optical band gaps in the UV region, these are found to be approximatively at 26000 cm^{-1} (3.3-3.2 eV) for all TiO_2 samples. The NIR range is dominated by a monotonic absorption entirely due to the scattering of the IR beam and dependent on the average particle size. The MIR range is dominated by an intense (out of scale) absorption due to bulk vibrations, whose edge is located at higher frequency for nanorutile and nanoanatase (1150 cm^{-1}), with respect to P-25 (1000 cm^{-1}).

Upon H_2 reduction at 500 °C (light grey curves) all TiO_2 samples became bluish in color, as testified by the appearance of intense bands in the visible-NIR region of the spectra (parts a), c) and e)) and lost most of the transparency in the MIR region (parts b), d) and f)), providing an evidence that shallow-trap defects are formed. However, the position of the absorption bands due to defects is different in the three cases. In particular, H_2-reduced nanoanatase (Fig. S1 part b)) shows a pronounced absorption at frequencies lower than 3500 cm^{-1}. On the contrary, H_2-reduced nanorutile loses transparency at wavenumbers higher than 3500 cm^{-1} (Fig S1 part d)), showing a maximum at 8000 cm^{-1} in the NIR region. This significant shift in the absorption maxima suggests that the majority of defect sites formed in nanorutile are hollow into the bulk of TiO_2, forming electronic states closer to the valence band. Finally, the spectrum of H_2-reduced Degussa P-25 (Fig S1 part f)) is more similar to that of nanoanatase; this observation should not surprise, since the rutile phase accounts for only the 15 % of the whole sample.

The spectra of all H_2-reduced samples show a slow decrease of Drude absorption in the MIR region upon contact with ethylene (last spectra reported in dark grey in Fig. S1). The gain in transparency is accompanied by the growth of polyethylene (as already discussed in the main text). These two simultaneous phenomena can be attributed to the reoxidation of a fraction of Ti^{4-n} surface species. On the contrary, almost no changes are observed in the Vis-NIR range of the spectra suggesting that the reoxidation involves only Ti^{4-n} defect sites close to the conduction band (surface sites) and not those more profound. Indeed, all samples maintain the blue color typical of the reduced Ti sites also after ethylene polymerization and turn to white only when are brought into contact with O_2.

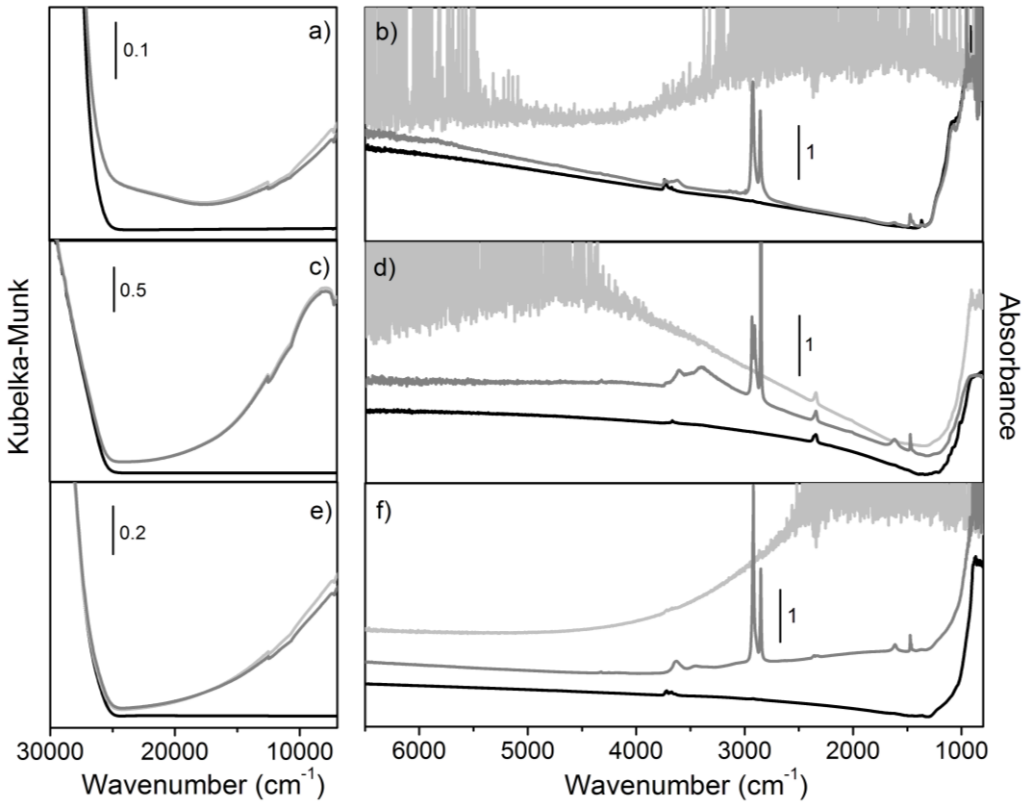

Figure S1: DRUV-Vis (parts a), c) and e)) and FT-IR (parts b), d) and f)) spectra of nanoanatase (a and b), nanorutile (c and d) and P-25 (e and f). Black curves show TiO_2 samples oxidized at 500 °C; the respective H_2 reduced samples are reported with light grey curves; and spectra shown in dark grey reveal the same samples upon 12 hours of reaction with ethylene gas phase.

2. Characterization of TiO_2/PE composites and of PE: a HR-TEM, SEM and DSC study

From the previous FT-IR studies it is possible to follow in-situ the polymerization of ethylene at the surface of TiO_2, but not to identify its morphology. HRTEM images (Fig. S2 and Fig. 2 in the main text) give important information on this topic, revealing the presence of a polymer casually grown on the oxide particles. Indeed, all oxide/polymer composites show the formation of lumps of polyethylene disposed randomly on the surface of TiO_2. The absence of a layer of polymer covering each particle of the oxides and the presence of spot-like polymerization cores suggest the formation of only a small fraction of peculiar surface Ti centers active in ethylene polymerization. HRTEM images show a different amount of polymeric product, which is indicative of the ability to form Ti reduced species active in ethylene polymerization on different phases. Among all TiO_2 samples, we have observed a higher quantity of polymeric products for reduced nanoanatase/polyethylene composites (Fig. S2 parts a) and b)); whereas reduced nanorutile phase exhibits only traces of polymer, nearly visible in the micrographs (Fig. S2 parts c) and d)). These data show the higher tendency of anatase phase to form active Ti reduced centers for ethylene polymerization.

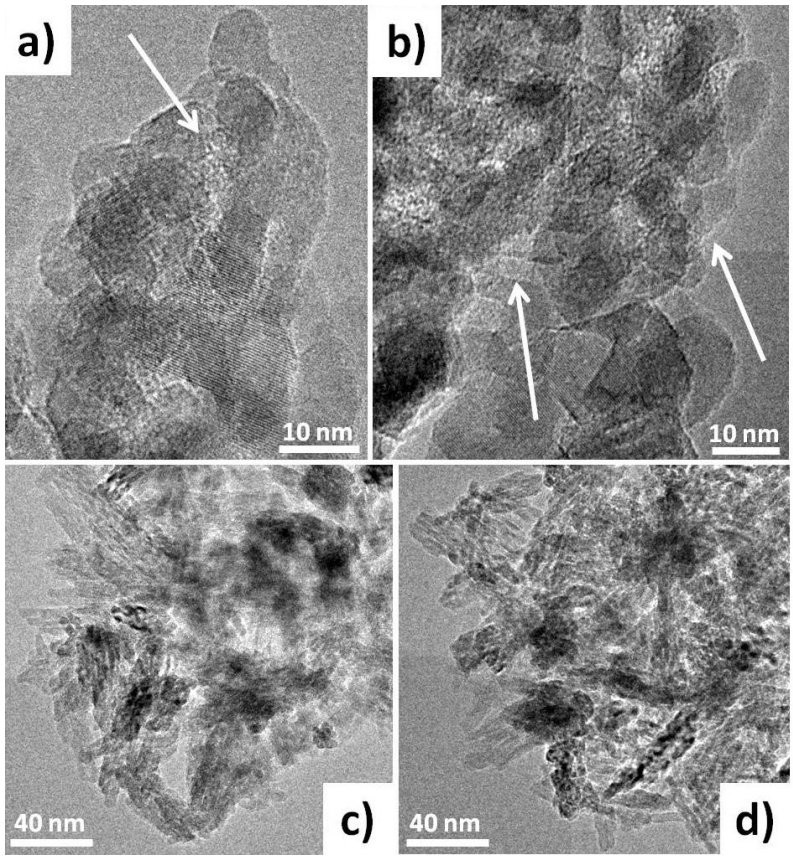

Figure S2: HRTEM micrographs of polyethylene-nanoanatase (parts a) and b)) and -nanorutile (parts c) and d)) composites revealing the presence of polyethylene (evidenced with white arrows) as random phase on the surface of the oxides.

In order to analyze the properties of the so obtained polyethylene the nanoanatase/PE composite was attacked by concentrated HF. This procedure cannot be repeated on the other 2 composites, because unfortunately HF dissolves only anatase phase and not rutile one. Figure S3 shows SEM images, in secondary and backscattered electrons, of PE extracted from the H_2 reduced nanoanatase sample. SEM images show the formation of PE agglomerates of 10 - 100 μm size, characterized by small protrusions. Shape and size distribution of the polymer particles is heterogeneous, as point out by higher enlargements (Fig S3 b) and c)). In many regions of the sample are also present filaments of PE connecting different polymer particles, as shown in Fig S3 c. From the images obtained with backscattered electrons (Fig S3 d)), it was possible to confirm the presence of the same composition phase throughout the sample, confirming a correct extraction of the polymer from the inorganic oxide phase.

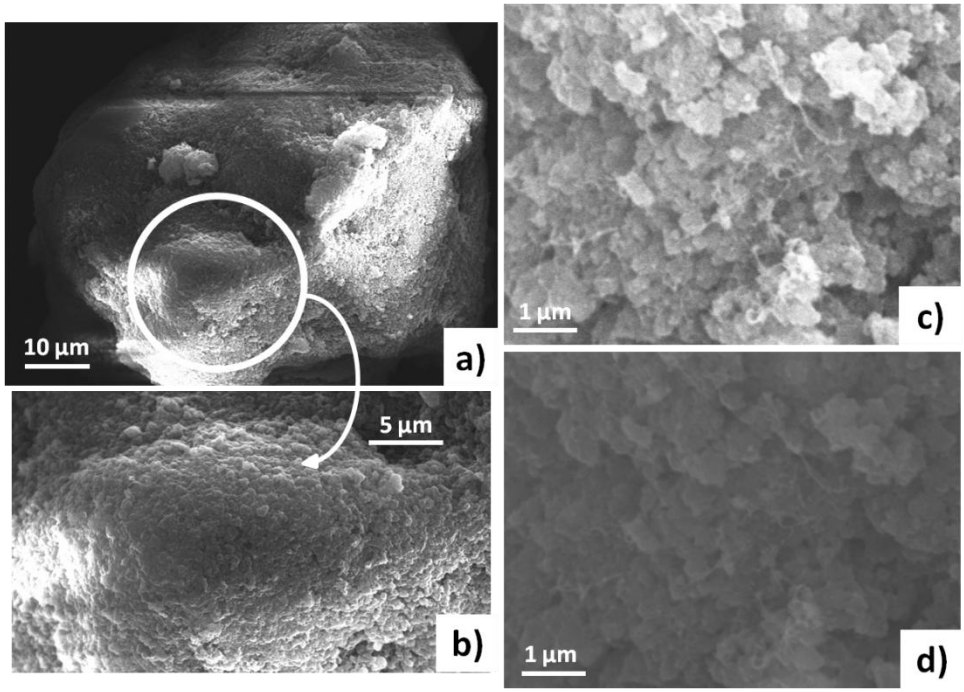

Figure S3: SEM images of PE extracted from H_2 reduced nanoanatase sample. Three different enlargements are shown from the lowest (part a)), until the highest (part c)). Part d) shows a backscattered electron image of the same region seen in part c).

The DSC curve of PE recovered after ethylene polymerization on H_2-reduced nanoanatase sample is shown in Figure S4 (samples of 7–12 mg were placed in closed aluminum pans and heated with a ramp of 2 °C/min in the temperature range from 50 to 150 °C; in Figure S4 is shown the second heating ramp). The melting temperature, higher than 130 °C, confirms the formation of High Density Polyethylene (HDPE) with a negligible level of branching, in agreement with the absence of IR absorption bands characteristic of CH_3 groups in the corresponding FT-IR spectrum, typically present when ramification occurs.

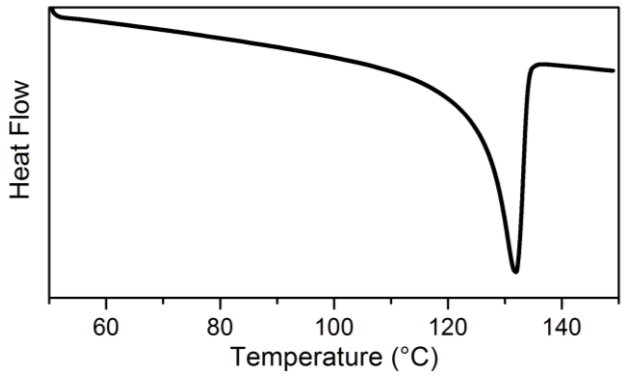

Figure S4: DSC curve of PE produced with nanoanatase reduced in H_2 atmosphere.